ChemCatChem

Research Article
doi.org/10.1002/cctc.202200549

Chemistry Europe
European Chemical Societies Publishing

www.chemcatchem.org

Catalytic Hydrogenolysis of Lignin into Phenolics by Internal Hydrogen over Ru Catalyst

Md. Anwar Hossain,[a] Tinnakorn Saelee,[b] Sarttrawut Tulaphol,[c] Mohammad Shahinur Rahaman,[a] Thanh Khoa Phung,[d] Thana Maihom,[e] Piyasan Praserthdam,[b] Supareak Praserthdam,*[b] Daniel J. Yelle,*[f] and Noppadon Sathitsuksanoh*[a]

Lignin is a by-product of biorefineries and pulp and paper manufacturers. Lignin is a renewable source of phenolic precursors for fuels and chemicals. Hydrogenolysis of lignin cleaves the abundant β-O-4 bonds and releases phenolics. However, selective hydrogenolysis of lignin's β-O-4 bonds is challenging because it requires high-pressure H_2. Here we show efficient hydrogenolysis of lignin model compounds and technical lignin by Ru/C catalyst and internal hydrogen. The aliphatic hydroxyl groups (C_α–OH) in lignin enabled Ru-catalyzed dehydrogenation of internal hydrogen and the formation of reactive keto intermediate, which facilitated the β-O-4 cleavage into phenolic monomers. Furthermore, solvents that had a high donor number (Lewis basicity) enhanced the yield of phenolic monomers, equal to 27.9 wt.% from technical lignin. These findings offer a novel approach for biorefineries to design lignin isolation processes and/or solvent systems to maximize phenolic monomers and to control product selectivity/stability.

Introduction

Production of fuels and chemicals from renewable lignocellulose has the potential to mitigate climate change and promote the bioeconomy.[1–3] Lignin accounts for 15–30 wt.% of lignocellulose.[4] The global production of lignin was 100 million tonnes/year in 2015 and is estimated to reach 225 million tonnes/year by 2030.[5] Lignin is a renewable feedstock for phenolics, and the ability to valorize lignin into phenolics would promote profitable biorefineries and bioeconomy. However, its complex chemical structure makes lignin difficult to fragment. Thus, lignin is regarded as waste[6–8] or used in low-value applications, such as low-grade solid fuel, concrete additives, animal feed pellets, and drilling muds.[9–11] Improved catalytic strategies are required to upgrade lignin.

Lignin consists of three major phenolic units, *p*-hydroxyphenyl (H), guaiacyl (G), and syringyl (S),[12–13] that are linked by C–O bonds (β-O-4) and C–C bonds (β-β'and β-5).[14–15] Cross-linking of these phenolic units creates a recalcitrant lignin matrix. Among these linkages, β-O-4 linkages are ~40-60% of total lignin linkages.[16–17] Therefore, to produce high yields of phenolic chemicals, it is necessary to efficiently cleave lignin's β-O-4 linkages to release phenolic monomers.[18]

Catalytic transfer hydrogenolysis of lignin is one of the most efficient strategies to break C_β–O bonds of β-O-4 linkages.[19–29] This approach uses hydrogen donor solvents as hydrogen sources[30–33] and transition metal catalysts, such as Pd,[34–36] Mo,[37–38] and Ni,[39–42] (Table S1). For example, Wang et al.[43] reported a low yield of phenolic monomers (10 wt.%) from hydrogenolysis of enzymatically derived corncob lignin by MOF-derived MoC catalysts in ethanol at 300 °C for 4 h. Matsagar et al.[44] used an Rh/C catalyst to hydrogenolyze alkaline lignin in ethanol-water at 250 °C with formic acid as hydrogen donor; the investigators obtained 3 wt.% monomer products. Moreover, added hydrogen pressure (20–30 bar) improved the yield of phenolic monomers. For example, Wang et al.[45] obtained 44.1 wt.% monomers from hydrogenolysis of Eucalyptus lignin with Pd/C in methanol at 180 °C and 30 bar H_2. Shu et al.[46] used Pd/C and $CrCl_3$ in methanol at 300 °C and 20 bar H_2 and obtained 26.3 wt.% monomer yield from lignin isolated by acid hydrolysis of sorghum straw. Li et al.[47] used

[a] M. A. Hossain, M. S. Rahaman, Prof. N. Sathitsuksanoh
Department of Chemical Engineering
University of Louisville
Louisville, KY 40292
(USA)
E-mail: n.sathitsuksanoh@louisville.edu
Homepage: http://tikgroup.org
[b] Dr. T. Saelee, Prof. P. Praserthdam, Prof. S. Praserthdam
Department of Chemical Engineering
Chulalongkorn University
Bangkok, 10330 (Thailand)
E-mail: supareak.p@chula.ac.th
[c] Prof. S. Tulaphol
Department of Chemistry
King Mongkut's University of Technology Thonburi
Bangkok 10140 (Thailand)
[d] Prof. T. K. Phung
School of Biotechnology
International University
Vietnam National University
Minh City 700000 (Vietnam)
[e] Prof. T. Maihom
Department of Chemistry
Kasetsart University
Nakhon Pathom 73140 (Thailand)
[f] Dr. D. J. Yelle
United States Department of Agriculture
Madison, WI 53726 (USA)
E-mail: daniel.j.yelle@usda.gov

Supporting information for this article is available on the WWW under https://doi.org/10.1002/cctc.202200549

Ru/C and Cs_2CO_3 in methanol to hydrogenolyze enzymatic mild acidolysis lignin (EMAL) from birch wood at 220 °C and 30 bar H_2 and obtained 27.4 wt.% monomer yield. Although added H_2 enabled high monomer yields, molecular hydrogen (H_2) poses safety concerns.[48] Moreover, molecular hydrogen is typically produced by steam reforming of fossil fuels with CO_2 as a by-product,[49–50] a contributor to greenhouse gas and climate change. As a result, the use of molecular hydrogen in lignin conversion is not a sustainable practice. Instead, we should develop catalytic hydrogenolysis systems that provide a high phenolic monomer yield without using external H_2.

Lignin molecules are good sources of hydrogen from their backbones, hydroxyl, and methoxyl groups.[48] The use of internal hydrogen from lignin molecules as hydrogen sources for catalytic transfer hydrogenation will simplify the lignin conversion process and eliminate the use of molecular hydrogen and/or hydrogen donor solvents. The result will be an efficient lignin conversion pathway without side reactions from solvents and without greenhouse gas emission. Previous studies support catalytic release of lignin's internal hydrogen for lignin conversion. For example, Zhou et al.[36] proposed that lignin and lignin model compounds underwent direct cleavage of the β-O-4 bonds with a Pd/C catalyst and dioxane as a hydrogen donor solvent at 160–180 °C. de Andrade et al.[51] used quantum calculations and showed that Pd catalysts catalyzed hydrogenolysis of lignin model compounds by dehydrogenation and keto-enol tautomerization prior to the β-O-4 bond cleavage. The enol tautomer from lignin model compounds caused polymerization into undesired products.[47] Li et al.[47] reported that Ru catalysts suppressed the formation of enol tautomer and side reactions (coke). Previously, we showed the hydrogenolysis ability of Ru/C on lignin model compounds in ethanol and dioxane as hydrogen-donor solvents without external H_2.[52] Although Ru-derived catalysts have been used for hydrogenolysis of lignin and lignin model compounds,[52–54] the mechanism whereby internal hydrogen promotes Ru-catalyzed hydrogenolysis of lignin's β-O-4 bonds was unknown. The lack of this information slows the efficient production of phenolics from lignin for biorefineries.

Here, we report the hydrogenolysis of lignin model compounds and technical lignin by an Ru/C catalyst in protic and aprotic solvents. We demonstrated that the C_α–OH groups enabled Ru-catalyzed dehydrogenation of the lignin model compound into a keto intermediate and facilitated the β-O-4 cleavage at 280 °C in both protic and aprotic solvents. Density Functional Theory calculations suggested that the dehydrogenation of C_α–H and C_α–OH into the keto intermediate was the key step for efficient hydrogenolysis. Further, we found that alcohols as hydrogen-donor solvents enabled the Meerwein–Ponndorf–Verley reduction of the keto product by RuO_x in the Ru/C catalyst and facilitated subsequent hydrodeoxygenation and hydrogenation to hydrocarbons. We used this information to hydrogenolyze four technical lignin samples. Hydrogenolysis of steam-exploded yellow poplar lignin gave the greatest phenolic yield of 27.9 wt.% in ethanol at 280 °C after 24 h. The fundamental understanding gained from this work will enable the design of efficient catalytic systems to maximize the phenolic yields from lignin for biorefineries.

Results and Discussion

Effect of C_α-hydroxyl groups on the cleavage of lignin model compounds by Ru/C under various hydrogen sources

Effect of C_α-OH groups on hydrogenolysis activity

To evaluate the importance of C_α-OH, we performed conversion of three model β-O-4 compounds, 2-phenyl ethyl phenyl ether (PPE, 1a), 2-phenoxy-1-phenylethanol (PPE-OH, 1b), and veratrylglycerol-β-guaiacyl ether (VGE, 1c), with Ru/C catalyst in 2-butanone under N_2 (Figure 1). PPE (1a) does not have C_α-OH, whereas PPE-OH (1b) and VGE (1c) contain C_α-OH. We chose 2-butanone because it was not a hydrogen-donor solvent. Heating these model compounds with Ru/C catalyst in 2-butanone under N_2 differed in reactant conversion. With PPE, we observed little to no conversion, whereas PPE-OH and VGE showed conversions of ~69-88% with 59% and ~99% selectivities to aromatic monomers, respectively. Phenol (4) and acetophenone (5) were major products from PPE-OH (1b). Guaiacol (6) and 1,2-dimethoxy-4-propenylbenzene (7) were major products from VGE (1c). These products suggested that PPE-OH (1b) and VGE (1c) underwent hydrogenolysis, and the methoxy groups in VGE (1c) did not hinder the reactivity to hydrogenolysis. Moreover, the unreactivity of PPE (1a) suggested that C_α-OH was critical in the enhanced reactivity of

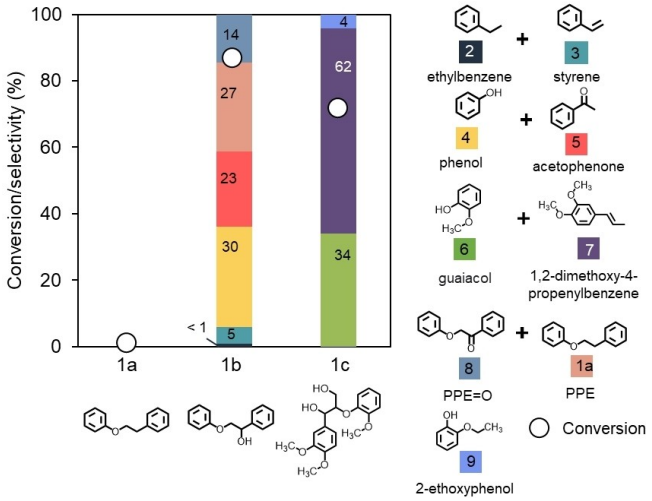

Figure 1. Cleavage of β-O-4 linkages of veratrylglycerol-β-guaiacyl ether (1c), 2-phenoxy-1-phenylethanol (1b), and 2-phenyl ethyl phenyl ether (1a) by Ru/C in 2-butanone under N_2. Reaction condition: 280 °C, 8 bar N_2, 1 wt.% reactant/2-butanone, 20 wt.% catalyst loading, 4 h. Hydrogenolysis of PPE-OH (1b) yielded 88% conversion with < 1% ethylbenzene (2), 5% styrene (3), 30% phenol (4), 23% acetophenone (5), 14% PPE=O (8), and 27% PPE (1a) selectivities. VGE yielded 69% conversion with 34% guaiacol (6), 62% 1,2-dimethoxy-4-propenylbenzene (7), and 4% 2-ethoxyphenol (9) selectivities. See Figure S2 for MS trace of products 6 and 7. Values in the bars indicate product selectivities.

model β-O-4 compounds for hydrogenolysis by Ru/C catalyst without hydrogen-donor solvents or addition of H_2.

Effect of alcohols on hydrogenolysis activity

To determine the effect of alcohols as hydrogen-donor solvents, we conducted hydrogenolysis by Ru/C catalyst in ethanol under N_2 with PPE (1a), PPE-OH (1b), and VGE (1c) (Figure S1A). PPE (1a) was not reactive to hydrogenolysis by Ru/C catalyst. Previous studies by Zhu et al.[55] performed hydrogenolysis of benzyl phenyl ether, a lignin model compound without C_α-OH, using Ru/C catalyst in methanol at 120 °C for 2 h. They observed no hydrogenolysis activity. Their findings were in agreement with our results on PPE (1a). However, heating PPE-OH (1b) and VGE (1c) with Ru/C catalyst in ethanol resulted in cleavage of the β-O-4 bond. PPE-OH (1b) yielded 55% conversion with 79% selectivities to aromatic monomers. The ethylbenzene (2) and styrerne (3) selectivities (34%) in ethanol suggested that ethanol promoted hydrodeoxygenation and hydrogenation reactions. Hydrogenolysis of VGE (1c) by Ru/C in ethanol yielded 99% conversion with 90% selectivities to aromatic monomers. These results suggested that (1) C_α-OH had a crucial function in the hydrogenolysis of the β-O-4 bond, and (2) the hydrogen-donor solvent (ethanol) was not necessary.

Effect of molecular hydrogen on hydrogenolysis activity

Next, we performed the same hydrogenolysis of PPE (1a) and PPE-OH (1b) in H_2 by the Ru/C catalyst (Figure S1B). Under H_2, we obtained 89% PPE-OH conversion under H_2 with 68% selectivities to aromatic monomers, a greater conversion than under N_2 (55%). These results suggested that added H_2 enhanced the rates of β-O-4 bond hydrogenolysis by Ru/C. Interestingly, under H_2, we obtained 51% conversion of PPE (1a, without C_α-OH) with 25% selectivities to aromatic monomers, compared with no activity under N_2. Previous studies showed hydrogenolysis activity of benzyl phenyl ether, a lignin model compound without C_α-OH, by Ru-based catalysts under H_2. For example, Cao et al.[54] performed hydrogenolysis of benzyl phenyl ether in methanol with Ru/C at 160 °C. They found that added H_2 (5–15 bar) enhanced conversion of benzyl phenyl ether and aromatic monomer yields. Similarly, Ji et al.[56] observed an enhanced yield of aromatic monomers from increasing H_2 pressure (from 1 to 7 bar) using Ru–W/C catalysts. Jiang et al.[57] reported an increase in aromatic monomer yield by Ru@ZIF-8 catalyzed hydrogenolysis of benzyl phenyl ether with increasing H_2 pressure (1–10 bar). Results from previous studies agreed well with our enhanced hydrogenolysis activity of PPE (1a, without C_α-OH) by Ru/C catalyst under H_2. Together, our results confirmed that the C_α–OH group was important in activating the hydrogenolysis of the β-O-4 bond without molecular H_2.

Because Ru catalysts are oxophilic and enable the formation of RuO_2, we performed hydrogenolysis of these three model β-O-4 compounds with RuO_2 catalyst in 2-butanone and ethanol under N_2 as a control (Figure S3, see *Supporting Information* for detail). RuO_2 in ethanol was active for hydrogenolysis of the β-O-4 bond, whereas the RuO_2 catalyst was not active in 2-butanone. Together, our results suggested that both metallic Ru and the C_α-OH were important in hydrogenolysis of the β-O-4 bond without external hydrogen sources (molecular H_2 and/or hydrogen-donor solvents).

Charge analysis and adsorption energy of reactant on Ru(0001) surface and stability of intermediates

To determine how the C_α–OH group promoted β-O-4 hydrogenolysis, we performed a charge analysis using charge density differences (CDD) and the Bader charge analysis to investigate the adsorption stability of PPE and PPE-OH on the Ru(0001) surface (Figure S4). We constructed the model Ru surface based on the hexagonal close-packed structure (Ru(0001) surface) because it had the lowest surface energy,[58–59] which suggested that the Ru(0001) surface was thermodynamically stable. Moreover, the Ru(0001) surface was reported as an active facet that strongly interacted with hydrogen species,[59–61] facilitating the hydrogenolysis, hydrogenation, and dehydrogenation steps. The positive and negative Bader charge change values (ρ) describe electron gain and loss during an adsorption process. During PPE and PPE-OH adsorption, the electron depletion from the top Ru(0001) surface and electron accumulation around carbon atoms of the benzene rings suggested that strong adsorption of PPE and PPE-OH took place by electron transfer from the Ru(0001) surface to the two benzene rings of PPE and PPE-OH. Moreover, in the case of PPE, a shorter atomic distance between O1 of PPE and the Ru(0001) surface indicated another contact point between PPE and the Ru(0001) surface apart from the benzene rings, which resulted in stronger adsorption between the PPE molecule and the Ru(0001) surface (Table S2).

Compared with PPE adsorption on Ru(0001), PPE-OH adsorption increased the distance between the O1 atom and the Ru(0001) surface and decreased the distance between H1 and Ru(0001). These changes suggested that the -OH reduced the O1-Ru(0001) interaction and promoted the H1-Ru(0001) interaction (which was weaker than the O1-Ru interaction).[62] Furthermore, the Bader charge analysis suggested that the Ru(0001) surface acted as an electron donor to the adsorbed PPE and PPE-OH. A higher electron gain of the PPE-OH molecule ($+2.17\,|e|$) indicated that the PPE-OH was more active than PPE. Interestingly, most electron gain on the PPE-OH was located around the H1 atom, whereas the electron gains were dispersed throughout the PPE molecule. Thus, we postulated that the electron accumulation at the H1 atom of PPE-OH promoted the dehydrogenation of the PPE-OH molecule. This dehydrogenation step of H1 in PPE-OH was essential to the O1-C1 bond activation (β-O-4 cleavage), and this step corroborated previous findings.[63–65] We speculate that the undetected O1-C1 bond cleavage in PPE was due to the lack of this dehydrogenation step.

To test the aforesaid hypothesis, we investigated the O1-C1 activation (β-O-4) mechanism in PPE and PPE-OH using their stable configurations and calculated the adsorption energy of

the proposed reaction step (*see Supporting Information and Figure S5 for detail*). The results suggested that the C_α-OH group in PPE-OH promoted the dehydrogenation of H1 and formed an intermediate (**Int B**) before hydrogenolysis of β-O-4 bonds into keto product (acetophenone) and phenol. These calculations agreed well with the hydrogenolysis results of lignin model compounds (Figure 1). To confirm the dehydrogenation of PPE-OH into **Int B** intermediate, we performed Bader charge analysis of PPE-OH on the Ru(0001) surface (Figure S6). The results suggested that the hydroxyl group at C_α induced electron accumulation at the H1 and created the active H1 during adsorption on Ru(0001) surface (**Int B**). The electron accumulation was around the H(O) atom of **Int B** (Figure 2), the H atom at the hydroxyl group, which suggested that (1) this H atom was active and (2) potential dehydrogenation of Int B into other intermediates. Because we expected the dehydrogenation of **Int B** intermediate into keto and enol tautomers, we calculated the adsorption energies of intermediates on the Ru(0001) surface (Figure S7). Their adsorption energy (E_{ads}) on the Ru(0001) surface was −4.93 eV for enol, −5.18 eV for keto, and −4.95 eV for **Int B**. These results disproved our hypothesis and suggested that either (1) both Int B and enol intermediates were not thermodynamically stable and converted to keto, or (2) the Ru-catalyzed hydrogenolysis pathway did not involve keto-enol tautomerization. Overall, our quantum calculation indicated that the C_α–OH group of PPE-OH activated its initial dehydrogenation and promoted electron accumulation at the H(O) atom of the hydroxyl groups to form keto-enol intermediates and facilitate the subsequent β-O-4 cleavage.

Effect of solvent on the formation of keto intermediate and β-O-4 bond cleavage of lignin model compounds

To evaluate the effect of the reaction solvent on β-O-4 cleavage, we performed hydrogenolysis of PPE-OH by the Ru/C catalyst under N_2 in (1) aprotic solvents (ethyl acetate, and 2-butanone) and (2) protic solvents (dioxane, ethanol, 1-propanol, 2-propanol, and 2-butanol) (Figure 3). The Ru/C catalyst was active for hydrogenolysis of PPE-OH (1b) in both aprotic and protic solvents at 280 °C for 4 h, with the conversion of PPE-OH greater than 50% in all solvents. Thus, hydrogen donor solvents

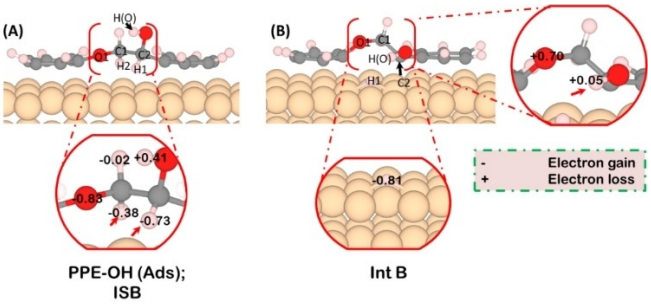

Figure 2. The atomic Bader charge of adsorption of (A) PPE-OH (ISB) and (B) intermediate B (Int B) states. The positive and negative signs represent electron gain and loss, respectively.

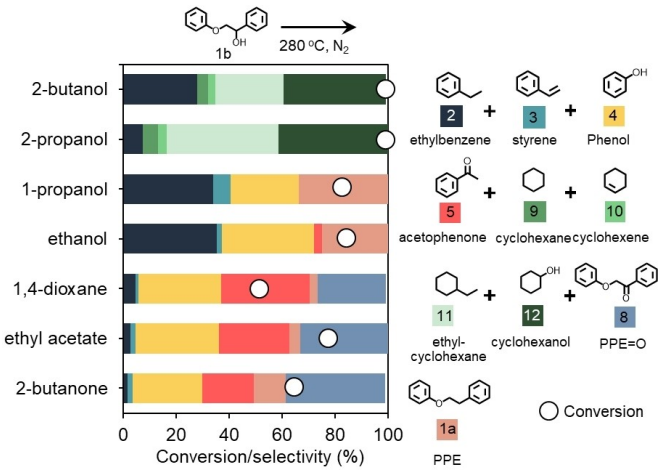

Figure 3. Cleavage of the β-O-4 bond of 2-phenoxy-1-phenylethanol (PPE-OH, 1b) by Ru/C in selected protic and aprotic polar solvents. Reaction condition: 280 °C, 4 h, 8 bar N_2, 1 wt.% 2-phenoxy-1-phenylethanol/solvent, 20 wt.% catalyst loading.

(protic solvents) were not necessary for hydrogenolysis by the Ru/C catalyst under the experimental conditions. In aprotic solvents (ethyl acetate and 2-butanone), major product selectivities were phenol (4), acetophenone (5), and PPE=O (8) with a small amount of ethylbenzene (2) and styrene (3). The presence of phenol (4) and acetophenone (5) suggested the β-O-4 cleavage in aprotic solvents. The small amount of ethylbenzene (2) and styrene (3) suggested the absence of hydrodeoxygenation in aprotic solvents.

Reactions by Ru/C catalyst in dioxane yielded products similar to those in aprotic solvents. One reason for similar products was that dioxane has a low donor number; thus dioxane had behavior similar to aprotic solvents. We monitored the evolution of reaction products in dioxane for 12 h. The conversion of PPE-OH (1b) and selectivity to β-O-4 cleavage increased with time (Figure S8). PPE=O was rapidly formed as shown by an increase in selectivity of PPE=O and a maximum of 29% at 20% PPE-OH conversion within the first 2 h. The selectivity of PPE=O was volcano-shaped, which suggested that PPE=O was an intermediate product. The selectivity of PPE=O dropped with reaction times >2 h. Moreover, the decrease in PPE=O corresponded to increased phenol (4) and acetophenone (5) selectivities. These results suggested that PPE=O was an intermediate product and converted to phenol and acetophenone. These results corroborated our computational studies and suggested that PPE=O was the keto intermediate from dehydrogenation of PPE-OH. Moreover, the selectivity toward the sum of ethylbenzene (2) and styrene (3) was low (i.e., $\Sigma 2+3=$ 7%), which suggested that Ru/C catalysis in dioxane proceeded with minimal side reactions (hydrodeoxygenation and hydrogenation) compared with reactions in protic solvents.

Reactions by Ru/C catalyst in primary alcohols (ethanol and 1-propanol) yielded phenol (4), ethylbenzene (2), and PPE (1a). Interestingly, we did not observe PPE=O as our reaction product.

To explain the product selectivity, we performed our reaction in 1-propanol between 230–250 °C. We observed an increase in selectivity of phenol (4) and the sum of ethylbenzene and styrene (Σ2 + 3) with increasing reaction temperature from 230 to 250 °C. The selectivity of PPE=O decreased with increasing temperature. We did not observe PPE=O with a reaction temperature of 280 °C. However, we observed the saturated aromatic products. These results suggested that PPE=O was formed in 2-propanol. However, the elevated temperature (> 250 °C) facilitated the ether cleavage of PPE=O into monomers (Figure S9A). Moreover, reaction temperature > 250 °C enhanced hydrodeoxygenation and/or hydrogenation of these resulting monomers into saturated phenolic and aromatic products as evidenced by an increase in HDO selectivity (Figure S9B).

Among protic solvents, reactions of PPE-OH with the Ru/C catalyst in 2-propanol and 2-butanol resulted in 100 % conversion of PPE-OH to ethylbenzene (2) and saturated aromatic products, cyclohexane (9), cyclohexene (10), ethyl cyclohexane (11), and cyclohexanol (12). The saturated aromatic products indicated that hydrogenolysis products underwent hydrodeoxygenation and hydrogenation. The secondary alcohols, 2-propanol and 2-butanol, were more effective hydrogen donors than primary alcohols (ethanol and 1-propanol).[66–67] Hence, we observed ring saturation products when we used 2-propanol and 2-butanol.

To explain the solvent effect on the hydrogenolysis activity of Ru/C catalyst, we plotted the phenolic monomer yield as a function of solvent properties, such as polarity, donor number, and acceptor number (Figure S10). The donor number indicates solvent Lewis basicity, and the acceptor number is a measure of the Lewis acidity of solvents. We obtained a good linear relationship between donor number and monomer yields (Figure S10C). The high monomer yield from reactions in a solvent with a high donor number suggested that a solvent with a high Lewis basicity enhanced the hydrogenolysis efficiency of PPE-OH by Ru/C catalyst. For example, we obtained 39 % monomer yield from the reaction in dioxane (low donor number), whereas the reaction in 2-butanol yielded 99 % monomers. These results suggested that the Lewis basicity of the solvents controlled the catalytic activity and product selectivity of the Ru catalyst. Wang et al.[42] showed that solvent with a high donor number (high Lewis basicity) blocked the active sites of Raney Ni in hydrogenolysis of diphenyl ether, a finding that contradicts our results.

Meerwein–Ponndorf–Verley (MPV) reduction initiated hydrodeoxygenation

Because we expected that the high selectivities of ethylbenzene (2) and styrene (3) in alcohols (Figure 3) were from the Meerwein–Ponndorf–Verley (MPV) of the acetophenone (keto product, 5), a hydrogenolysis product of lignin model compound, we performed similar experiments using Ru/C catalyst and acetophenone (5) as the reactant in 2-butanone and ethanol. We selected these solvents as proxies for aprotic and protic solvents. As expected with 2-butanone, we did not have any catalytic activity (< 3 %) (Table 1). In contrast, we had 24 % acetophenone conversion in ethanol after 0.5 h. We observed three reaction products, ethylbenzene (2), styrene (3), and 1-phenylethanol (5*). The presence of ethylbenzene and styrene suggested that the hydrodeoxygenation of acetophenone occurred only in protic solvents. The presence of 1-phenylethanol suggested the occurrence of MPV reduction. Moreover, we observed a decrease in benzyl alcohol yield and an increase in ethylbenzene yield with time. These results indicated that 1-phenylethanol underwent hydrodeoxygenation into styrene and subsequent hydrogenation into ethylbenzene.

To explain the inactivity of Ru/C catalyst in acetophenone conversion in 2-butanone, we performed reactions using RuO_2 (Table S4). With 2-butanone, we did not observe any products, whereas we observed 1-phenylethanol (5*) from RuO_2 in ethanol. These results suggested the in-situ generation of active sites of RuO_2 in ethanol for MPV by reduction. We postulated that these active sites were oxygen vacancies (RuO_x). The Ru catalysts' oxophilic nature enables the formation of RuO_x oxygen vacancies under a reducing environment, such as alcohols.[68–70] These RuO_x oxygen vacancies are active sites for MPV reduction. Jae et al.[71] reported that partially oxidized Ru/C and reduced RuO_2 catalysts were effective for the MPV reaction of 5-hydroxymethylfurfural to 2,5-bis(hydroxymethyl)furan in propanol, which suggested that the formation of defects (oxygen vacancies) enabled MPV reduction. Mironenko et al.[70] and Gilkey et al.[68] further explained that RuO_x oxygen vacancies catalyzed MPV reduction of furfural to furfuryl alcohol in 2-propanol, which corroborated DFT calculations by Jenness et al.[72] The RuO_x catalyzed direct intermolecular hydride transfer from alcohol to furfural, a finding that agrees with our results.

To confirm the in-situ generation of oxygen vacancies in Ru/C catalyst in ethanol, we performed H_2-TPR on the used catalysts after reaction (stored under N_2 to prevent oxidation). As a control, our fresh catalyst contained 41 % RuO_2 (Ru/RuO_2 ratio = 1.4, Table S5). The Ru/RuO_2 ratio of the used catalyst in 2-butanone was 1.5, a value similar to that of fresh catalyst. Whereas used catalysts in ethanol had an increased Ru/RuO_2 ratio (3.8). Thus, RuO_2 was reduced in ethanol and formed

Table 1. Acetophenone conversion by Ru/C in ethanol and 2-butanone

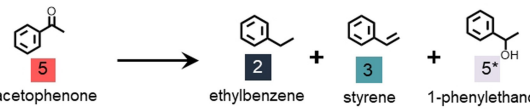

Solvent	Time [h]	Conversion [%]	Selectivity [%]		
			2	3	5*
Ethanol	0.5	24	58	4	22
	1.0	33	77	5	18
	2.0	73	83	4	2
	0.5	< 5	–	–	–
	1.0	< 5			
2-butanone	2.0	< 5	–	–	–

Reaction condition: 280 °C, 4 h, 8 bar N_2, 1 wt.% 2-phenoxy-1-phenylethanol/solvent, 20 wt.% catalyst loading. HDO extent = sum of 2 and 3 selectivities. MPV extent = the sum of ethylbenzene (2), styrene (3), and 1-phenylethanol (5*).

oxygen vacancies. We expected that the oxygen vacancies were the active sites for the MPV reaction of acetophenone to styrene. To test this hypothesis, we reduced fresh Ru/C catalyst in ethanol for 12 h to generate oxygen vacancies prior to adding acetophenone (Table S6). As a control, the fresh Ru/C catalyst had 73.1% MPV extent (1.2% 1-phenylethanol, 3.0% styrene, and 68.9% ethylbenzene yields). The pre-reduced Ru/C catalyst showed only 25.5% MPV extent. This low MPV extent was due to a high Ru/RuO_2 (10.5) of pre-reduced Ru/C catalyst, which resulted in low oxygen vacancies formed during the reaction. Together, MPV reduction of the keto product (acetophenone) in a hydrogen donor solvent (ethanol) by the oxygen vacancies (RuO_x) in Ru/C catalyst was a key step that led to hydrodeoxygenation and hydrogenation products. Hence, the choice of the solvent in Ru/C catalytic systems could be used to control product selectivity.[54,73–74]

Stability and reusability of the Ru/C catalyst

The ability to reuse catalysts is important for their practical use. After hydrogenolysis of PPE-OH in ethanol at 280 °C for 4 h (Figure 1), we recovered the Ru/C catalyst by centrifugation and washing with ethanol to remove the residual products, intermediates, and unreacted reactant. The catalyst was then placed in the reactor for reuse under the same hydrogenolysis condition. We observed a progressive decrease in the conversion of PPE-OH and changes in product selectivities over four reuses (Figure S11). One reason was that Ru is oxophilic. The RuO_2 species in the Ru/C catalyst was reduced in ethanol and formed oxygen vacancies, RuO_x (Figure S12). As a result, the used Ru/C catalyst in ethanol contained more metallic Ru content as the catalyst recycling progressed, which led to a decrease in conversion and changes in product selectivities. Another possible cause of the changes in the catalytic performance of the reused Ru/C catalyst in ethanol might have been due to metal aggregation, as evidenced by the occurrence of the (002) and (101) crystal planes of Ru at ~38.7 and 44.1°,[75–76] respectively (Figure S13).

Validation of hydrogenolysis by internal hydrogen with technical lignin

To validate the importance of the C_α–OH group in β-O-4 cleavage, we applied hydrogenolysis by Ru/C in 2-butanone to four types of technical lignin: (1) steam-exploded yellow poplar lignin (YL), (2) organosolv lignin (OL), (3) kraft lignin (KL), and (4) soda lignin (SL). Hydrogenolysis in ethanol yielded phenolic monomers from combined alkylguaiacols and alkylsyringols (Table S7). The YL lignin gave the highest monomer yield of 12.5 wt.% after 4 h, followed by KL > OL > SL. Interestingly, reactions in 2-butanone with the Ru/C catalyst for 4 h produced a total monomer yield similar to that in ethanol (Table S8). Prolonged reaction time from 4 to 24 h increased the total monomer yield to 20.2 wt.% in 2-butanone and 27.9 wt.% in ethanol (Figure 4), which mirrored the higher monomer yield from lignin model compounds in ethanol (Figure 3).

To assess the aging of the resulting monomers, we left the reaction products under the ambient condition and monitored changes in composition during 24 h (Tables S7 and S8). The reaction mixture in 2-butanone became darker and had a decreased total monomer yield. Whereas the reaction product in ethanol appeared more stable. These results suggested that, although hydrogen-donor solvent (ethanol) was not necessary for hydrogenolysis of lignin, a hydrogen-donor solvent stabilized the phenolic monomers. Huang et al.[77] reported that ethanol acted as a capping agent and suppressed char formation, a finding that agrees with our results.

To identify changes in molecular weight distribution of the lignin hydrogenolysis products, we performed size exclusion chromatography (SEC, Figure S14). The SEC chromatogram revealed a distinct change in molecular weight between kraft lignin and its hydrogenolysis products. The hydrogenolysis products of kraft lignin had a high intensity of bands in the range of 130–800 Da, which corroborated the molecular weight of identified phenolic monomers (Figure 4).

Because we expected that the foregoing monomer yield of 27.9 wt.% from YL lignin was due to its high C_α–OH and C_α=O concentrations, we performed HSQC NMR on technical lignin samples to determine the C_α–OH and C_α=O content (Figure S15). From the HSQC spectra of the technical lignin and the corresponding integral data (Table S9), the quantity of C_α–OH groups was the highest in the YL, closely followed by the KL and SL. The OL had the lowest amount of C_α–OH. The quantity of C_α=O groups was the highest in SL, followed by YL and KL. On the basis of the percent of the sum of the integrals for C_α, YL had the highest total integral, followed by KL, SL, and OL (*see Supporting Information for determination of C_α–OH and C_α=*

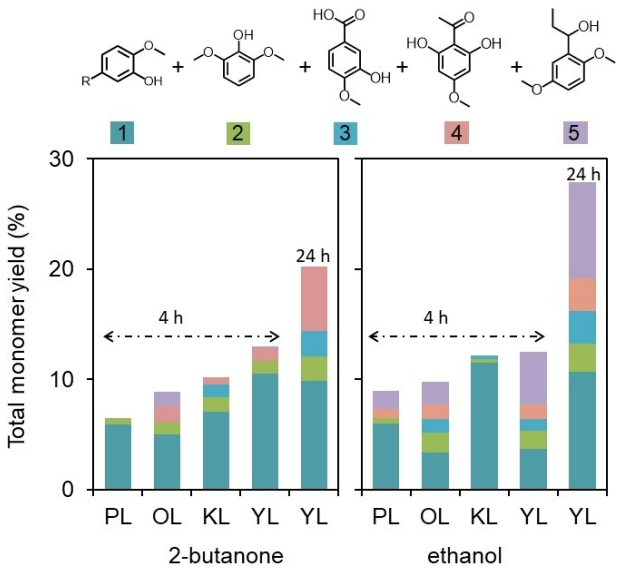

Figure 4. Hydrogenolysis of the technical lignin over Ru/C catalyst in 2-butanone and ethanol under N_2 for 4 h. Reaction condition: 280 °C, 8 bar N_2, 1 wt.% lignin, 20 wt.% catalyst loading, 4 h. R = –H, $–CH_3$, $–CH_2CH_3$, and $–CH_2CH_2CH_3$.

O contents in β-O-4 subunits of technical lignin by NMR (Tables S9 and S10)).

Interestingly, the ranking of the total C_α integral was in the order of YL > KL > SL > OL, the same order as the order of hydrogenolysis yield. Because YL had a higher C_α integral than other lignins, YL provided greater monomer yields. These results substantiated the importance of C_α–OH groups in the cleavage of the β-O-4 bond. Surprisingly, although KL had a high sulfur content of 0.9 wt.%, the hydrogenolysis yield of KL in ethanol at 24 h was 24 wt.%, greater than the hydrogenolysis yields of OL and SL, which had only 0.2-0.3 wt.% sulfur. Sulfur typically poisons metal catalysts, such as Pt, Co, and Ni.[78–80] Thus, the Ru catalyst appeared to be sulfur-tolerant.

Proposed chemical pathway of breaking lignin by Ru/C

Together with computational results, we postulated the chemical pathway of hydrogenolysis of technical lignin by Ru/C (Figure 5). The C_α–OH enabled the dehydrogenation at the C_α–H and then C_α–OH groups by Ru catalysts into the keto intermediate (C_α=O) for subsequent β-O-4 cleavage to keto and alcohol products; the reactions occurred without hydrogen-donor solvents and/or external H_2 gas. Previous studies showed that the enol intermediate was important in lignin degradation reactions under alkaline,[81–82] acid,[83–84] and/or transition metal catalysts.[34,85–86] Galkin et al.[34] proposed that transfer hydrogenolysis of model lignin β-O-4 compounds by Pd/C in ethanol with base (ethylamine, diethylamine, ammonia, and polymer-supported amine) and formic acid as a hydrogen donor solvent, formed keto intermediate after the dehydrogenation step and followed by the keto-enol tautomerization before subsequent β-O-4 cleavage to monomers. By quantum calculations, de Andrade et al.[51] confirmed the keto-enol tautomerization in the hydrogenolysis pathway by Pd/C. In the case of Ru catalysts, Li et al.[47] used Ru/C catalyst for hydrogenolysis of model lignin β-O-4 compounds in methanol and base (Cs_2CO_3, K_2CO_3, and CaOAc) under 20–30 bar H_2. They found that lignin hydrogenolysis by Ru catalyst proceeded by deprotonation of C_γ-OH and C_β-H. Moreover, the Ru catalyst suppressed the formation of enol intermediate, a result that contradicts our findings. The different hydrogenolysis pathways by Ru catalyst deduced by Li et al.[47] might have been due to the applied external H_2, which activated dehydrogenation from different locations of the lignin structure. Together, our results further confirmed that C_α–OH group of lignin facilitated the β-O-4 cleavage.

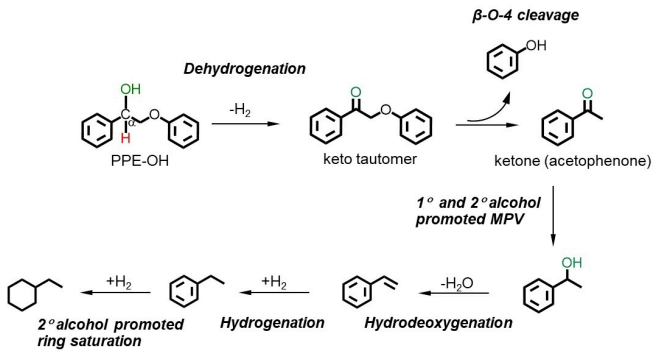

Figure 5. Proposed reaction pathway for conversion of model β-O-4 compounds with C_α–OH group by Ru/C catalyst

Conclusion

Selective hydrogenolysis of lignin is important for producing phenolics for fuels and chemicals. Most current hydrogenolysis processes use 10–30 bar H_2 to maximize the yield of phenolic monomers; the inclusion of H_2 raises safety concerns and contributes to capital and operational expenditures. Our findings advance the understanding of the hydrogenolysis of lignin in which the internal hydrogen was used to cleave β-O-4 linkages by Ru catalyst. Hydrogen donor solvents and external H_2 enhanced the hydrogenolysis activity and phenolic monomer yield of Ru catalysts, but these agents were unnecessary. Moreover, the mechanistic understanding gained from this work suggested that increasing the C_α–OH in technical lignin's structure would enhance the yield of phenolic monomers from hydrogenolysis by Ru catalyst without relying on external H_2 sources or hydrogen-donor solvents. This knowledge could guide development of isolation and functionalization steps to provide lignin with a high C_α–OH content for production of phenolic monomers for profitable biorefineries and the bioeconomy. Upcoming studies will focus on the effect of oxygen vacancies on the subsequent hydrodeoxygenation of hydrogenolysis products.

Experimental Section

Materials

Model β-O-4 compounds were 2-phenoxy-1-phenylethanol (PPE-OH),[20,87–88] 2-phenethyl phenyl ether (PPE),[89–91] and veratrylglycerol-β-guaiacyl ether (VGE).[92–94] PPE-OH and PPE contained C_α–OH and C_α–H, respectively. VGE had C_α–OH with methoxy substituted on the ring to represent the actual functional groups of technical lignin. The Ru/C catalyst was the commercial 5% supported Ru catalyst on activated carbon from Alfa Aesar (Haverhill, MA, USA) and stored in the glove box under Ar to avoid exposure to air. The amounts of metallic Ru and RuO_x were determined by integrating the H_2 consumption profile with respect to the H_2 standard. The Ru and RuO_2 were 59 and 41 wt.%, respectively. The pre-reduced Ru/C catalyst was used as a control. All reagents and catalysts were used as received unless otherwise noted. They were stored in a glove box to prevent oxidation. The manufacturers, purity, and CAS numbers are shown in Table S11.

Hydrogenolysis of lignin model β-O-4 compounds

All reactions were performed in a 25 mL autoclave reactor (Parr Instrument, Moline, IL, USA). The reactant concentration was ~1 wt.% of lignin model compounds in organic solvents, unless otherwise noted. The catalyst loading was 20 wt.% (~20 mg catalyst, 2 mol.% Ru) with respect to reactant (100 mg reactant in 10 g solvent solution). Before the reaction, the reactor was purged three times with N_2 to remove air. The reactor was then pressurized

to 8 bar N_2 or H_2 at ambient temperature to minimize the evolution of hydrogen and to maintain the consistency of the experiment. The hydrogenolysis reaction was performed at 280 °C for 4 h with a stirring rate of 600 rpm to minimize mass transfer limitation. The reaction was stopped by quenching in a cold water bath. The reaction sample was withdrawn, centrifuged to remove residual solids, and diluted with ethanol before product analysis.

Reaction product identification and quantification

Changes in reactants and products during the cleavage of β-O-4 bonds were identified and quantified by the Agilent 7890B GC (Agilent Technologies, Santa Clara, CA, USA) equipped with Mass spectrometry (MS) and Flame Ionization Detectors (FID). An HP-5MS column (30 m × 0.25 mm × 0.25 μm, Agilent Technologies, Santa Clara, CA, USA) was used for product separation with the following temperature program: injection temperature 275 °C and FID detector temperature 300 °C; split ratio 1:50. The temperature program started at 45 °C and increased at 10 °C/min to 250 °C, then held for 20 min. The change in reactant and products was determined with dodecane as the internal standard (*see Supporting Information for calculations*).

Characterization of catalysts

Selected catalysts were characterized by H_2-temperature-programmed reduction (H_2-TPR)[52] and X-ray diffraction (*see Supporting Information for detail*).

Characterization of technical lignin and lignin hydrogenolysis products

The technical lignin and lignin hydrogenolysis products were characterized by elemental analysis (CHONS),[95–97] Nuclear Magnetic Resonance (NMR),[98–99] and Size Exclusion Chromatography (SEC)[98–100] (*see Supporting Information for detail*).

Computational methods

To reveal the hydrogenolytic mechanism, we used the density functional theory (DFT) by creating the model Ru catalyst and lignin model compounds with the Vienna ab initio simulation package (VASP) Version 5.4.4.[101–104] The detailed information of computational parameters, model construction of the Ru surface, and optimized structures of model compounds (Figs. S16–S18 and Table S12), and Gibb free energy (ΔG) calculations are shown in *Supporting Information*.

Acknowledgements

A part of this material is based upon work supported by the National Science Foundation under Cooperative Agreement No. 1355438. This work was performed in part at the Conn Center for Renewable Energy Research at the University of Louisville, which belongs to the National Science Foundation NNCI KY Manufacturing and Nano Integration Node, supported by ECCS-1542174. We would like to thank Ingevity Corp., USA for kraft lignin. Also, we would like to thank Professors Scott Renneckar (University of British Columbia, Canada) and Wolfgang Glasser's (Virginia Tech, USA) laboratories for providing technical lignin samples. For the computational section, this research project is partially supported by the Second Century Fund (C2F), Chulalongkorn University. Authors would also like to acknowledge the computing facility from the High-Performance Computing Unit (CECC-HCU), Center of Excellence on Catalysis and Catalytic Reaction Engineering (CECC), Chulalongkorn University, Thailand. The authors would like to thank Dr. Howard Fried for his valuable comments and suggestions on the manuscript.

Conflict of Interest

The authors declare no conflict of interest.

Data Availability Statement

The data that support the findings of this study are available on request from the corresponding author. The data are not publicly available due to privacy or ethical restrictions.

Keywords: lignin · hydrogenolysis · Ru · dehydrogenation · Meerwein–Ponndorf–Verley · oxygen vacancies

[1] A. Chandel, V. Garlapati, S. Jeevan Kumar, M. Hans, A. Singh, S. Kumar, *Biofuels Bioprod. Biorefin.* **2020**, *14*, 830–844.
[2] A. Ubando, C. Felix, W.-H. Chen, *Bioresour. Technol.* **2020**, *299*, 122585.
[3] S. Hassan, G. Williams, A. Jaiswal, *Renewable Sustainable Energy Rev.* **2019**, *101*, 590–599.
[4] T. D. Bugg, M. Ahmad, E. M. Hardiman, R. Rahmanpour, *Nat. Prod. Rep.* **2011**, *28*, 1883–1896.
[5] D. Bajwa, G. Pourhashem, A. H. Ullah, S. Bajwa, *Ind. Crops Prod.* **2019**, *139*, 111526.
[6] W. Sangchoom, R. Mokaya, *ACS Sustainable Chem. Eng.* **2015**, *3*, 1658–1667.
[7] W. Liu, R. Zhou, H. Goh, S. Huang, X. Lu, *ACS Appl. Mater. Interfaces* **2014**, *6*, 5810–5817.
[8] M. Garedew, F. Lin, B. Song, T. DeWinter, J. Jackson, C. Saffron, C. Lam, P. Anastas, *ChemSusChem* **2020**, *13*, 4214–4237.
[9] S. Kang, X. Li, J. Fan, J. Chang, *Bioresour. Technol.* **2012**, *110*, 715–718.
[10] P. H. S. S. Moreira, J. C. de Oliveira Freitas, R. M. Braga, R. M. Araújo, M. A. F. de Souza, *Ind. Crops Prod.* **2018**, *116*, 144–149.
[11] K. E. B. Knudsen, *Anim. Feed Sci. Technol.* **1997**, *67*, 319–338.
[12] J. Ralph, G. Brunow, W. Boerjan, in *Encyclopedia of Life Sciences*, John Wiley & Sons Ltd, **2007**, p. doi: 10.1002/9780470015902.a9780470020104.
[13] R. Vanholme, B. Demedts, K. Morreel, J. Ralph, W. Boerjan, *Plant Physiol.* **2010**, *153*, 895.
[14] H. Kim, J. Ralph, *Org. Biomol. Chem.* **2010**, *8*, 576–591.
[15] H. Kim, J. Ralph, T. Akiyama, *BioEnergy Res.* **2008**, *1*, 56–66.
[16] Y. Zhu, Z. Han, L. Fu, C. Liu, D. Zhang, *J. Mol. Model.* **2018**, *24*, 322.
[17] J. Gierer, *Wood Sci. Technol.* **1980**, *14*, 241–266.
[18] J. Zakzeski, P. C. A. Bruijnincx, A. L. Jongerius, B. M. Weckhuysen, *Chem. Rev.* **2010**, *110*, 3552–3599.
[19] J. Zhang, X. Jiang, X. Ye, L. Chen, Q. Lu, X. Wang, C. Dong, *J. Therm. Anal. Calorim.* **2016**, *123*, 501–510.
[20] J. Lu, M. Wang, X. Zhang, A. Heyden, F. Wang, *ACS Catal.* **2016**, *6*, 5589–5598.
[21] C. Zhang, J. Lu, X. Zhang, K. MacArthur, M. Heggen, H. Li, F. Wang, *Green Chem.* **2016**, *18*, 6545–6555.
[22] W. Deng, H. Zhang, L. Xue, Q. Zhang, Y. Wang, *Chin. J. Catal.* **2015**, *36*, 1440–1460.
[23] M. Zaheer, R. Kempe, *ACS Catal.* **2015**, *5*, 1675–1684.
[24] Z. Luo, C. Zhao, *Catal. Sci. Technol.* **2016**, *6*, 3476–3484.
[25] Z. Luo, Y. Wang, M. He, C. Zhao, *Green Chem.* **2016**, *18*, 433–441.
[26] C. S. Lancefield, O. S. Ojo, F. Tran, N. J. Westwood, *Angew. Chem. Int. Ed. Engl.* **2015**, *54*, 258–262.

[27] B. Gómez-Monedero, M. P. Ruiz, F. Bimbela, J. Faria, *Appl. Catal. A* **2017**, *541*, 60–76.
[28] A. L. Jongerius, R. Jastrzebski, P. C. A. Bruijnincx, B. M. Weckhuysen, *J. Catal.* **2012**, *285*, 315–323.
[29] J. Zhang, G. Lu, C. Cai, *Green Chem.* **2017**, *19*, 4538–4543.
[30] C. Cheng, J. Truong, J. Barrett, D. Shen, M. Abu-Omar, P. Ford, *ACS Sustainable Chem. Eng.* **2019**, *8*, 1023–1030.
[31] X. Lu, H. Guo, J. Chen, D. Wang, A. Lee, X. Gu, *ChemSusChem* **2022**, *15*, e202200099.
[32] E. Paone, A. Beneduci, G. Corrente, A. Malara, F. Mauriello, *J. Mol. Catal.* **2020**, *497*, 111228.
[33] H. Wu, J. Song, C. Xie, C. Wu, C. Chen, B. Han, *ACS Sustainable Chem. Eng.* **2018**, *6*, 2872–2877.
[34] M. Galkin, S. Sawadjoon, V. Rohde, M. Dawange, J. Samec, *ChemCatChem* **2014**, *6*, 179–184.
[35] F. Gao, J. Webb, H. Sorek, D. Wemmer, J. Hartwig, *ACS Catal.* **2016**, *6*, 7385–7392.
[36] X. Zhou, J. Mitra, T. B. Rauchfuss, *ChemSusChem* **2014**, *7*, 1623–1626.
[37] L.-P. Xiao, S. Wang, H. Li, Z. Li, Z.-J. Shi, L. Xiao, R.-C. Sun, Y. Fang, G. Song, *ACS Catal.* **2017**, *7*, 7535–7542.
[38] S. Wang, W. Gao, H. Li, L. P. Xiao, R. C. Sun, G. Song, *ChemSusChem* **2018**, *11*, 2114–2123.
[39] Q. Song, F. Wang, J. Cai, Y. Wang, J. Zhang, W. Yu, J. Xu, *Energy Environ. Sci.* **2013**, *6*, 994–1007.
[40] I. Klein, B. Saha, M. Abu-Omar, *Catal. Sci. Technol.* **2015**, *5*, 3242–3245.
[41] X. Wang, R. Rinaldi, *Energy Environ. Sci.* **2012**, *5*, 8244–8260.
[42] X. Wang, R. Rinaldi, *ChemSusChem* **2012**, *5*, 1455–1466.
[43] Q. Wang, T. Su, Y. Wang, Y. Chen, X. Lu, R. Ma, Y. Fu, W. Zhu, *ACS Sustainable Chem. Eng.* **2020**, *8*, 17008–17015.
[44] B. Matsagar, Z. Y. Wang, C. Sakdaronnarong, S. Chen, D. Tsang, K. W. Wu, *ChemCatChem* **2019**, *11*, 4604–4616.
[45] S. Wang, W. X. Li, Y. Q. Yang, X. Chen, J. Ma, C. Chen, L. P. Xiao, R. C. Sun, *ChemSusChem* **2020**, *13*, 4548–4556.
[46] R. Shu, Q. Zhang, L. Ma, Y. Xu, P. Chen, C. Wang, T. Wang, *Bioresour. Technol.* **2016**, *221*, 568–575.
[47] H. Li, G. Song, *ACS Catal.* **2019**, *9*, 4054–4064.
[48] X. Shen, C. Zhang, B. Han, F. Wang, *Chem. Soc. Rev.* **2022**, *51*, 1608–1628.
[49] L. Barelli, G. Bidini, F. Gallorini, S. Servili, *Energy* **2008**, *33*, 554–570.
[50] A. Boyano, A. Blanco-Marigorta, T. Morosuk, G. Tsatsaronis, *Energy* **2011**, *36*, 2202–2214.
[51] A. de Andrade, P. Srifa, P. Broqvist, K. Hermansson, *ChemSusChem* **2020**, *13*, 6574–6581.
[52] M. A. Hossain, T. K. Phung, M. S. Rahaman, S. Tulaphol, J. B. Jasinski, N. Sathitsuksanoh, *Appl. Catal. A* **2019**, *582*, 117100.
[53] Y. Wu, Z. Lin, X. Zhu, X. Hu, M. Gholizadeh, H. Sun, Y. Huang, S. Zhang, H. Zhang, *Fuel* **2021**, *302*, 121184.
[54] J.-P. Cao, T. Xie, X.-Y. Zhao, C. Zhu, W. Jiang, M. Zhao, Y.-P. Zhao, X.-Y. Wei, *Fuel* **2021**, *284*, 119027.
[55] C. Zhu, J.-P. Cao, X.-Y. Zhao, T. Xie, M. Zhao, X.-Y. Wei, *Fuel Process. Technol.* **2019**, *194*, 106126.
[56] J. Ji, H. Guo, C. Li, Z. Qi, B. Zhang, T. Dai, M. Jiang, C. Ren, A. Wang, T. Zhang, *ChemCatChem* **2018**, *10*, 415–421.
[57] W. Jiang, J.-P. Cao, J.-X. Xie, L. Zhao, C. Zhang, C. Zhu, X.-Y. Zhao, Y. Zhao, J. Zhang, *Catal. Sci. Technol.* **2022**, *12*, 488–496.
[58] Y. Nanba, T. Ishimoto, M. Koyama, *J. Phys. Chem. C* **2017**, *121*, 27445–27452..
[59] K. K. Ghuman, K. Tozaki, M. Sadakiyo, S. Kitano, T. Oyabe, M. Yamauchi, *Phys. Chem. Chem. Phys.* **2019**, *21*, 5117–5122..
[60] C. J. Zhang, M. Lynch, P. Hu, *Surf. Sci.* **2002**, *496*, 221–230..
[61] J. A. Herron, S. Tonelli, M. Mavrikakis, *Surf. Sci.* **2013**, *614*, 64–74.
[62] Y.-R. Luo, *Comprehensive Handbook of Chemical Bond Energies*, 1st Edition ed., **2007**.
[63] J. M. Nichols, L. M. Bishop, R. G. Bergman, J. A. Ellman, *J. Am. Chem. Soc.* **2010**, *132*, 12554–12555.
[64] G. Zhu, X. Ouyang, L. Jiang, Y. Zhu, D. Jin, Y. Pang, X. Qiu, *Fuel Process. Technol.* **2016**, *154*, 132–138.
[65] C. Zhang, J. Lu, X. Zhang, K. MacArthur, M. Heggen, H. Li, F. Wang, *Green Chem.* **2016**, *18*, 6545–6555.
[66] K.-i. Fujita, T. Yoshida, Y. Imori, R. Yamaguchi, *Org. Lett.* **2011**, *13*, 2278–2281.
[67] Y. Ukisu, T. Miyadera, *React. Kinet. Catal. Lett.* **2004**, *81*, 305–311.
[68] M. J. Gilkey, P. Panagiotopoulou, A. V. Mironenko, G. R. Jenness, D. G. Vlachos, B. Xu, *ACS Catal.* **2015**, *5*, 3988–3994.
[69] P. Panagiotopoulou, N. Martin, D. G. Vlachos, *J. Mol. Catal. A* **2014**, *392*, 223–228.
[70] A. V. Mironenko, D. G. Vlachos, *JACS* **2016**, *138*, 8104–8113.
[71] J. Jae, W. Zheng, A. M. Karim, W. Guo, R. F. Lobo, D. G. Vlachos, *ChemCatChem* **2014**, *6*, 848–856.
[72] G. Jenness, D. Vlachos, *J. Phys. Chem. C* **2015**, *119*, 5938–5945.
[73] Y. Zeng, Z. Wang, W. Lin, W. Song, *Chem. Eng. J.* **2017**, *320*, 55–62.
[74] T. Walker, A. Motagamwala, J. Dumesic, G. Huber, *J. Catal.* **2018**, *369*.
[75] S. Tee, C. Lee, S. Dinachali, S. Lai, E. Williams, H.-K. Luo, D. Chi, T. Hor, M.-Y. Han, *Nanotechnology* **2015**, *26*, 415401.
[76] D. Austin, M. Jenkins, D. Allman, S. Hose, D. Price, C. Dezelah, J. Conley Jr, *Chem. Mater.* **2017**, *29*, 1107–1115.
[77] X. Huang, T. Korányi, M. Boot, E. Hensen, *Green Chem.* **2015**, *17*, 4941–4950.
[78] C. G. Visconti, L. Lietti, P. Forzatti, R. Zennaro, *Appl. Catal. A* **2007**, *330*, 49–56.
[79] J. Jones, V. Dupont, R. Brydson, D. Fullerton, N. Nasri, A. Ross, A. Westwood, *Catal. Today.* **2003**, *81*, 589–601.
[80] J. Hepola, P. Simell, *Appl. Catal. B* **1997**, *14*, 287–303.
[81] S. Kubo, J. Kadla, *J. Wood Chem. Technol.* **2008**, *28*, 106–121.
[82] S. Jia, B. Cox, X. Guo, Z. Zhang, J. Ekerdt, *Holzforschung* **2010**, *64*, 577–580.
[83] C. Lahive, P. Deuss, C. Lancefield, Z. Sun, D. Cordes, C. Young, F. Tran, A. Slawin, J. de Vries, P. Kamer, N. Westwood, K. Barta, *J. Am. Chem. Soc.* **2016**, *138*, 8900–8911.
[84] G. De Gregorio, C. Weber, J. Gräsvik, T. Welton, A. Brandt, J. Hallett, *Green Chem.* **2016**, *18*, 5456–5465.
[85] L. Shuai, M. Amiri, Y. Questell-Santiago, F. Héroguel, Y. Li, H. Kim, R. Meilan, C. Chapple, J. Ralph, J. Luterbacher, *Science* **2016**, *354*, 329–333.
[86] T. Lohr, Z. Li, T. Marks, *ACS Catal.* **2015**, *5*, 7004–7007.
[87] W. Deng, H. Zhang, X. Wu, R. Li, Q. Zhang, Y. Wang, *Green Chem.* **2015**, *17*, 5009–5018.
[88] J. Zhang, H. Asakura, J. van Rijn, J. Yang, P. Duchesne, B. Zhang, X. Chen, P. Zhang, M. Saeys, N. Yan, *Green Chem.* **2014**, *16*, 2432–2437.
[89] W. Guan, X. Chen, H. Hu, C.-W. Tsang, J. Zhang, C. Lin, C. Liang, *Fuel Process. Technol.* **2020**, *203*, 106392.
[90] L. Jiang, H. Guo, C. Li, P. Zhou, Z. Zhang, *Chem. Sci.* **2019**, *10*, 4458–4468.
[91] M. Klein, P. Virk, *Ind. Eng. Chem. Fundam.* **1983**, *22*, 35–45.
[92] A. Enoki, G. Goldsby, M. Gold, *Arch. Microbiol.* **1980**, *125*, 227–231.
[93] B. Cox, J. Ekerdt, *Bioresour. Technol.* **2012**, *118*, 584–588.
[94] S. Jia, B. Cox, X. Guo, Z. Zhang, J. Ekerdt, *Ind. Eng. Chem. Res.* **2011**, *50*, 849–855.
[95] M. Rahaman, S. Tulaphol, K. Mills, A. Molley, M. Hossain, S. Lalvani, T. Maihom, M. Crocker, N. Sathitsuksanoh, *ChemCatChem* **2022**, *14*, e202101756.
[96] M. Rahaman, S. Tulaphol, M. Hossain, J. Jasinski, N. Sun, A. George, B. Simmons, T. Maihom, M. Crocker, N. Sathitsuksanoh, *Fuel* **2022**, *310*, 122459.
[97] M. Rahaman, S. Tulaphol, M. Hossain, J. Jasinski, S. Lalvani, M. Crocker, T. Maihom, N. Sathitsuksanoh, *ChemCatChem* **2022**, *14*, e202200129.
[98] N. Sathitsuksanoh, M. Sawant, Q. Truong, J. Tan, C. G. Canlas, N. Sun, W. Zhang, S. Renneckar, T. Prasomsri, J. Shi, Ö. P. Çetinkol, S. Singh, B. A. Simmons, A. George, *BioEnergy Res.* **2015**, *8*, 973–981.
[99] N. Sathitsuksanoh, K. M. Holtman, D. J. Yelle, T. Morgan, V. Stavila, J. Pelton, H. Blanch, B. A. Simmons, A. George, *Green Chem.* **2014**, *16*, 1236–1247.
[100] A. George, K. Tran, T. J. Morgan, P. I. Benke, C. Berrueco, E. Lorente, B. C. Wu, J. D. Keasling, B. A. Simmons, B. M. Holmes, *Green Chem.* **2011**, *13*, 3375–3385.
[101] G. Kresse, J. Hafner, *Phys. Rev. B* **1994**, *49*, 14251.
[102] G. Kresse, J. Furthmüller, *Phys. Rev. B* **1996**, *54*, 11169.
[103] G. Kresse, J. Hafner, *Phys. Rev. B* **1993**, *47*, 558.
[104] J. Hafner, *Comput. Phys. Commun.* **2007**, *177*, 6–13.

Manuscript received: April 24, 2022
Revised manuscript received: August 17, 2022
Accepted manuscript online: August 25, 2022
Version of record online: September 26, 2022